A NOVEL BULK ACOUSTIC WAVE BASED SUPER-HARMONIC QUADRATURE VOLTAGE CONTROL OSCILLATOR

by

Arnab Jyoti Baruah

A dissertation submitted to the faculty of
The University of North Carolina at Charlotte
in partial fulfillment of the requirements
for the degree of Doctor of Philosophy in
Electrical Engineering

Charlotte

2022

Approved by:

_____
Dr. Jeremy Holleman

_____
Dr.Thomas Weldon

_____
Dr. Farid Tranjan

_____
Dr. Alan Dow

ABSTRACT

ARNAB JYOTI BARUAH . A Novel Bulk Acoustic Wave based Super-harmonic Quadrature Voltage Control Oscillator. (Under the direction of DR. JEREMY HOLLEMAN)

As the demand for wireless connectivity increases,new power and area efficient solutions will be required to meet the specifications of these systems. Most transceivers require a local oscillator with quadrature(I/Q) phases and the power and noise specifications of this oscillator plays a crucial role in the system performance. Although traditionally these oscillators were designed using on chip LC components, recent advances in manufacturing have opened the possibilities of incorporating Bulk Acoustic Wave(BAW) resonators in the design of such oscillators. In this work, we introduce a novel coupling technique for creating a Quadrature Voltage Controlled Oscillator(QVCO) which leads to a lower phase noise and power consumption compared to other published designs.

DEDICATION

This thesis is dedicated to my parents Krishna Jyoti Baruah and Indira Baruah

ACKNOWLEDGEMENTS

This thesis would not have been possible without the guidance of my advisor Jeremy Holleman.

I would also like to thank all my fellow graduate students and the faculty and staff members at University of Tennessee and UNC Charlotte without whose help the graduate school experience would have been incomplete. There were a lot of people who helped me in this journey so it wouldn't be possible to name everyone here but if you are reading this, you know who you are.

TABLE OF CONTENTS

LIST OF TABLES

LIST OF FIGURES

CHAPTER 1: INTRODUCTION

1.1 BACKGROUND AND MOTIVATION

The growing demand for wireless communications has led to new requirements in Transmitters and Receivers(Transceivers).In order to reduce equipment size and cost, highly integrated. The performance of any architecture depends on the what specification are achievable from the building blocks, so it is very important that these building blocks are optimised to get the most performance for a given power and area budget.This gives us the motivation to explore new circuit ideas.

One such circuit that almost every electronic system uses, is the Voltage Controlled Oscillator. Most wireless receivers, use one of the two basic receiver front end architectures:

- Super-Heterodyne:The incoming signal is down converted to an Intermediate frequency(IF) and then another demodulation stage is used to extract the information from the IF signal.

- Homodyne:The RF signal is down converted to base-band in one stage with the local oscillator being at the same frequency as the incoming signal.

The drawback with super-heterodyne receivers(SHR) is that both the incoming RF signal and the image frequency(which is an unwanted input frequency equidistant from the local oscillator frequency but opposite sign from the desired input RF signal) is that both the image frequency and the desired RF are down-converted to the IF(as shown in figure 1.1). This issue can be avoided by adding an image reject filter but this demands the use of components with very tight specifications. They are generally external components and make the system larger. This can be however be eliminated

by using the quadrature signals in the mixer (Hartley and Barber-Weaver) [8] . These receivers are called Image Reject Receivers(IRR)

Although Homodyne Receivers(HR) are not subject to this issue, they are sensitive to parasitic baseband disturbances and to 1/f noise. These receivers are also called Zero-IF(ZIF) receivers.

We can also combine the best of both the architectures above called the Low-IF receiver(LIFR). This is in principle a Superheterodyne Receiver with a combination of image rejection and low IF.

The choice of the architecture is based on the standard that is being designed for. For example some standard such as the GSM/DCS/PCS/EDGE have been designed using SHR, LIFR and HR. Bluetooth implementations mostly use a low-IF whereas multi standards such 802.11a/b/g use the Zero-IF architecture.

The oscillator plays the role of an important building block in the design of these receivers. Although the output of the oscillator can be just one phase, most architectures require the use of 2 quadrature phases. Quadrature signals are two identical periodic signals, quater of a period apart in time and are required to obtain the image cancellation in IRR. For FSK and PSK demodulation using the ZIF, quadrature signals are required for the mixer as well.

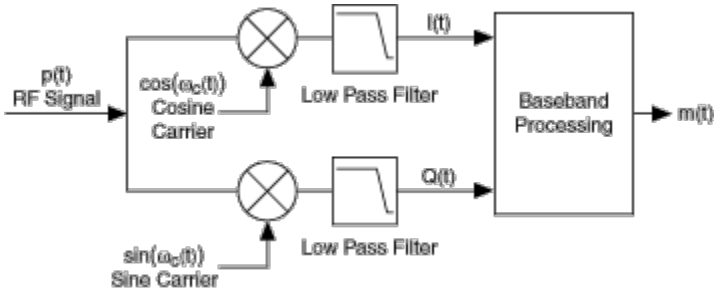

Figure 1.1: Direct Conversion Receiver

A Primary specification for the Oscillator is the phase noise. As it will be shown later, this determines the ability of the receiver to detect a weak signal in the pass band in the presence of a strong in-band blocker, a feature which is very important

in wireless systems where multiple agents share the same channel. The oscillator is therefore also responsible for the system to be able to operate in different bands within the given bandwidth of the transceiver. Hence the ability of a VCO to deliver quadrature signals within a power budget and good phase noise performance is critical for the operation of any communication system.

Besides being used in receiver front end circuits,these quadrature oscillators also find use in providing phase interpolation for phased-array transceivers and for creating clock phases for half-rate clock and data recovery (CDR) circuits.

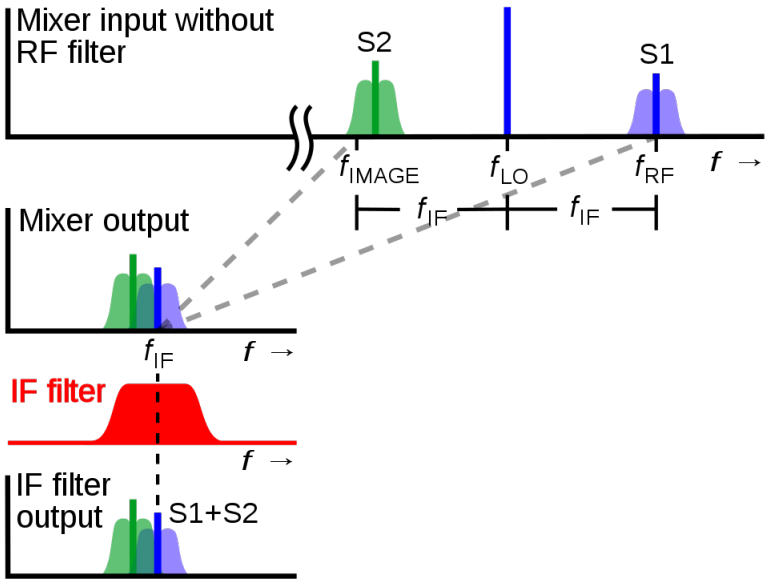

Figure 1.2: Image problem in Superheterodyne Receiver

Generation of quadrature signals with good power and phase noise performance presents an interesting challenge for the designer of wireless systems. Oscillators that are used for this purpose are a topic of active research. More importantly it is important to achieve good quadrature accuracy as well as low phase noise noise at the same time.

1.2 QUADRATURE SIGNAL GENERATION

Quadrature signal generation can be accomplished through several methods. They are briefly described below

1.2.1 POLYPHASE FILTERS

They are constructed by splitting the signal into two paths. Each path consists on a RC network. The top path is a RC network whereas the bottom path is a CR network.The phase shift at DC for the top network is 0° whereas the phase shift for the bottom network at DC is +90°. As we increase the frequency the phase shift of the top network starts decreasing to -90° whereas the phase shift in the bottom network starts decreasing towards 0°.

Although the phase shift of each branch varies with frequency,the phase difference between the branches is always 90°.

One limitation of this approach is that the amplitude does vary with frequency. The outputs are only equal at a certain frequency given by ω_p=1/RC

At ω_p, phase shift in the top network is +45° whereas the other path has -45° of phase shift.

Although it is straightforward to set ω_p as the frequency of oscillations. There is 3dB attenuation and there is thermal noise generated in the network. Besides that, mismatch between the RC components leads to phase errors.

Since the poly-phase filters are created using passive elements i.e. resistors and capacitors, in order to drive the resistive loads it is required that the VCO output has to be buffered. These buffers bring up the power consumption of the system.

In order to reduce the power consumption in the buffers the resistance has to be increased. This however means that the corresponding capacitance values have to be reduced(RC time constant is set by frequency of oscillations). Reducing the capacitance makes it more sensitive to parasitics.This becomes a problem as we go

to higher frequencies as both R and C become smaller with increasing frequency.

Due to these limitations other quadrature techniques may be used which offer a better phase and amplitude relationship.

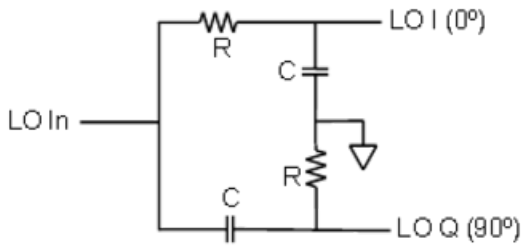

Figure 1.3: Single ended Polyphase filter

1.2.2 DIVIDE-BY-2 FREQUENCY DIVIDERS

Another method of generating quadrature signals is by employing frequency division. This techniques involves the use of a master slave flip flop pair to divide the frequency of a oscillator(which runs at double the desired frequency). If the duty cycle of the incoming reference frequency is 50% the phase difference between the output of the two flip flops is 90°.

Although this method of generation of quadrature signals is pretty straightforward, the local oscillator has to work at twice the frequency. As we go higher up in frequency,the power consumption in the local oscillators goes up too. This limits the maximum achievable frequency of operation.

The other drawback to this approach is that the two latches have to be laid out in a way to minimize mismatch between them which might lead to phase error.

1.2.3 QUADRATURE OSCILLATORS

Two identical oscillators can be made to operate in quadrature by coupling the outputs of one oscillators to the other oscillator using a coupling port as seen in Figure 1.5

A typical implementation of this circuit would look like Figure 1.6

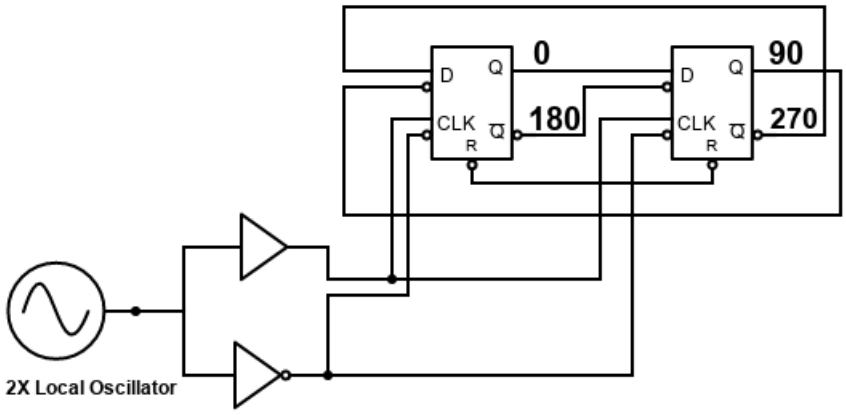

Figure 1.4: Divide by 2 Quadrature generation

In this case the coupling is created using another differential pair that is used to sense the output voltage of the first oscillator and inject a current into the tank of the second circuit.

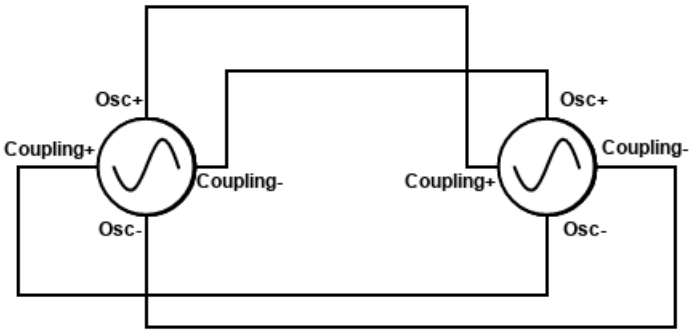

Figure 1.5: Quadrature Oscillator Architecture

The equivalent linear model in Fig1.7 can be used to calculate the phase difference between the oscillators.

For the circuit to sustain oscillations,it has to satisfy Barkhausen's criteria. This also means that the total phase change around the loop will be 2π. For simplicity if we assume the phase contributed by each coupling transconductance is 0 and π respectively. Since the tanks will behave identically and each contribute a phase shift

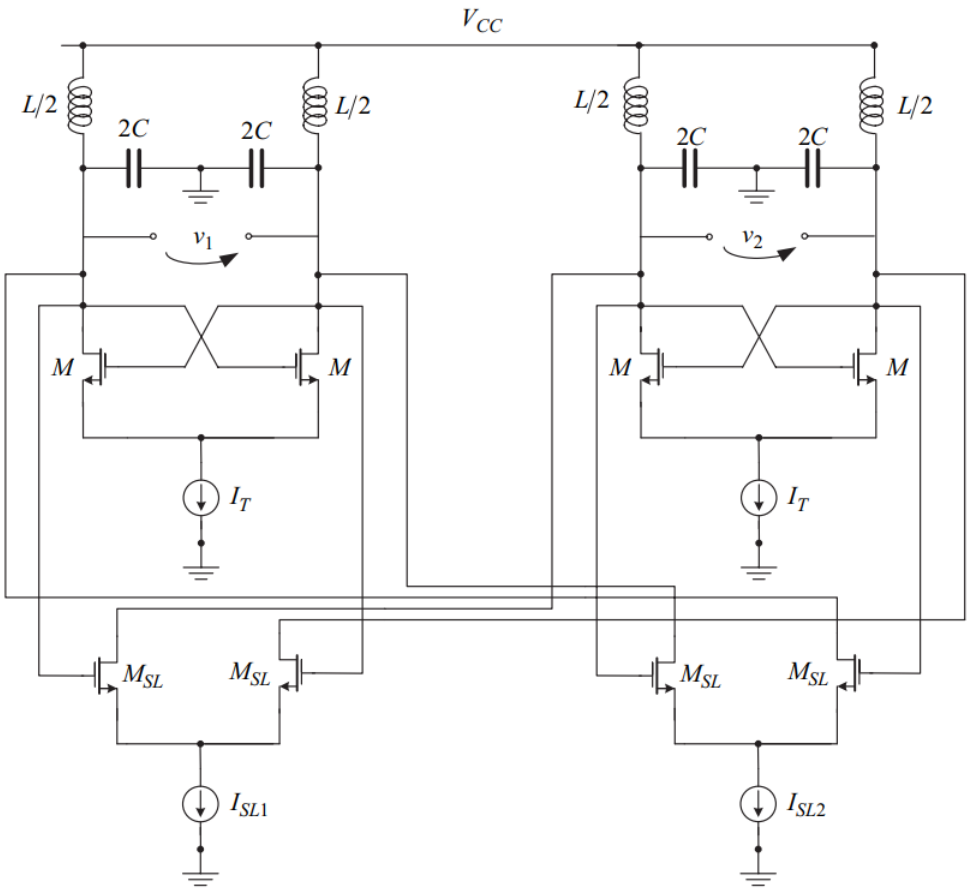

Figure 1.6: LC Quadrature Oscillator

which we will assume to be Φ, we can write the total phase shift around the loop as

$$0 + \pi + 2\Phi = 2\pi$$

which leads to

$$\Phi = \pi/2$$

This can also be visualised using the phasor diagram as shown in Figure 1.8

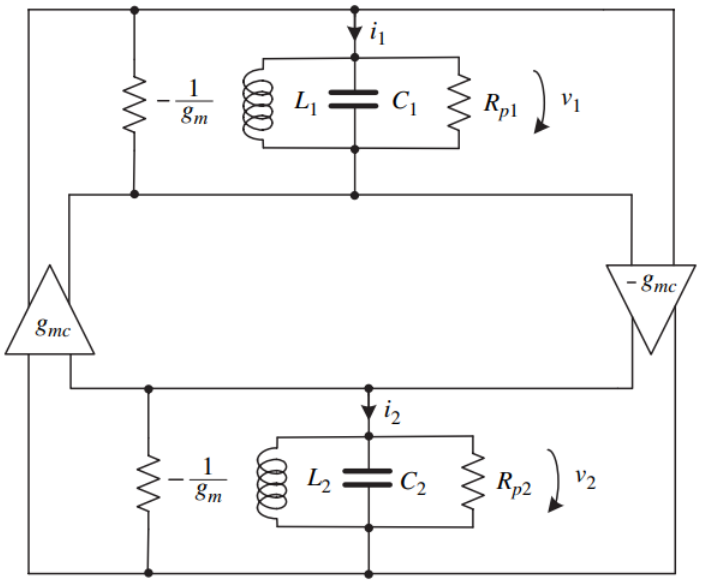

Figure 1.7: Linear model of Quadrature Oscillator

It can be shown that the frequency of oscillation can be approximated as

$$\omega_{osc} \approx \omega_o \pm \frac{g_{mc}}{2C}$$

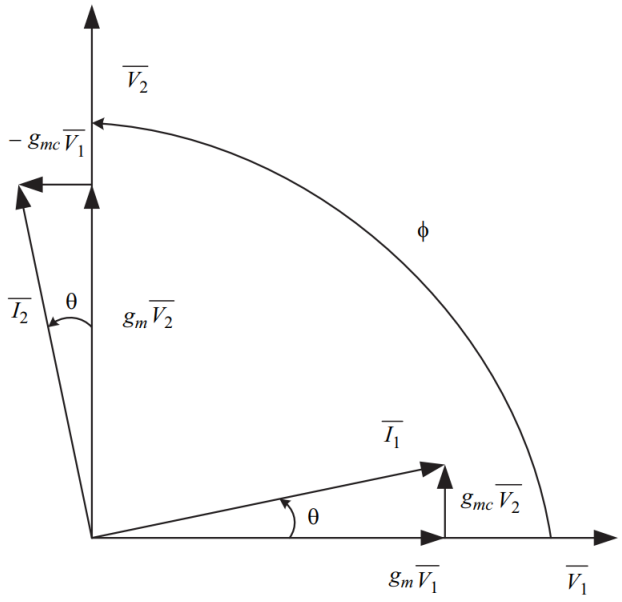

Figure 1.8: Phasor diagram of Quadrature oscillator

The oscillator will oscillate at one of these frequencies and it has observed through measurements that it is often the lower of the frequencies that the system locks in.

Although it is relatively popular, the oscillators designed using this method suffer from poor phase noise as the tank circuit works off resonance.

1.2.3.1 SUPER-HARMONICALLY COUPLED QUADRATURE VCO

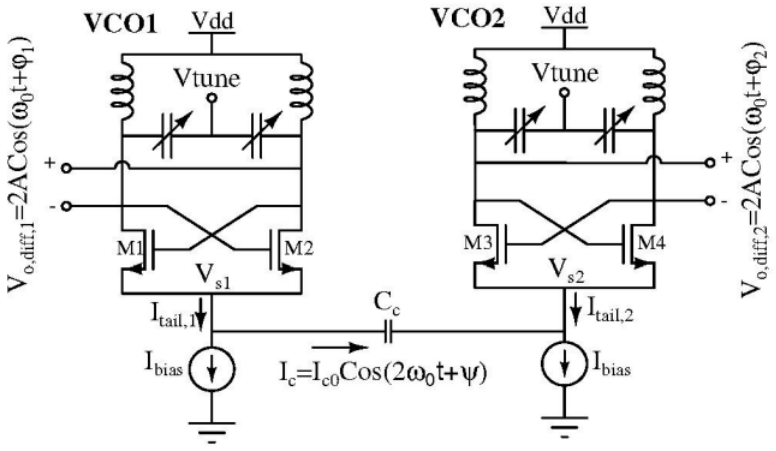

Figure 1.9: Super harmonic Oscillator

The alternate way to couple harmonic signals uses the second harmonic frequency which lets the tank work at resonance and this results in better phase noise.

As can be seen from Figure 1.9, instead of coupling through fundamental nodes, quadrature locking can be realized by enforcing a 180° phase difference between the second harmonics extracted from the IQ oscillator common-mode nodes [9].

This anti-phase relationship between the two second harmonics can be achieved by either using an on chip transformer [10], using a second harmonic oscillator or a frequency doubling circuit [11]. Although these methods allow to establish a quadrature phase lock between the two oscillator cores, the transformer adds extra die area whereas the second harmonic oscillator and the frequency doubling circuit require that addition of extra active devices which lead to the additional noise in the system.In the quest to achieve cost efficiency(silicon area) and better performance(lower

phase noise), new circuit designs will have to be investigated.

1.3 THESIS MOTIVATION AND STRUCTURE

BAW oscillators, which will be introduced in the next chapter, are different from their LC counterparts due to the inherent differences in the equivalent circuit and this leads to a different biasing scheme in order for them to satisfy stability conditions. These differences brings about new challenges in designing coupling networks for quadrature oscillators built using these devices.

In this work we introduce a novel technique to couple the second harmonic signal by exploiting the inherent passive biasing network so as to minimise the use of extra devices. As per our best knowledge, this is the first documented work that demonstrated the use of this technique for use in Bulk Acoustic Wave(BAW) based oscillators.

We begin by looking at BAW Resonators and Oscillators based on these Resonators(Chapter 2) and how super-harmonic coupling works(Chapter 3), followed by the analysis of the Proposed circuit(Chapter 4) and simulations results(Chapter 5). We conclude(Chapter 6) with key results from the proposed design.

CHAPTER 2: BAW BASED OSCILLATORS

In this chapter we look at some oscillator topologies that have been published in the literature over the years. Although the first such oscillator can be traced way back to 1976 [12], BAW oscillators have not been used in commercial products until 2019.

We first discuss the resonator model and then take a look at some oscillators and compare the performances.

2.1 BAW RESONATOR

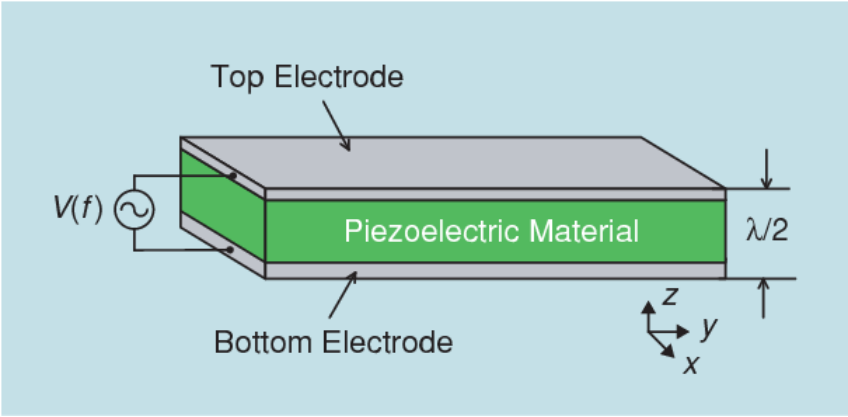

Figure 2.1: BAW Resonator Cross section

A BAW resonator is a passive structure designed by using piezoelectric material like Aluminum Nitride(AlN) and connected by two electrodes Figure 2.1. The resonant frequency is a function of the AlN thickness and the ability of make high frequency resonators is primarily limited by the ability to grow thin films.

The resonant frequency can be expressed as

$$f_0 = v/2d$$

where f_0 is the resonant frequency,v is the acoustic velocity and d is the thickness of the piezoelectric

For such a resonator, the piezoelectric coupling is a measure of how effectively energy is transformed from mechanical to electrical domain and vice versa. Resonators with higher coupling have lower losses.

2.1.1 BAW RESONATOR MODEL

For BAW resonators, two parameters of interest are the Quality factor(which is an indicator of how capable the resonator is in its ability to store energy during one cycle of operation) and the electromagnetic coupling co-efficient (k_{eff}^2) , which represents the effectiveness of the resonator in its ability to convert mechanical energy to electrical energy and vice-versa. Based on these, we define a Figure of Merit as the following

$$FOM = k_{eff}^2.Q$$

where the Q is the quality factor and k_{eff}^2 is the effective coupling coefficient, which also gives the bandwidth information, is defined as [13]

$$k_{eff}^2 = \frac{\pi^2.f_s.(f_p - f_s)}{4.f_p^2}$$

It is to be noted that k_{eff}^2 is not the same as k_t^2 which is the piezoelectric material coupling co-efficient. If the material has sufficiently high k_t^2, a resonator with the required k_{eff}^2 can be designed [14]. Other factors that effect k_{eff}^2 are the acoustic reflector, electrode configuration and the parasitics [15] [16].

In terms of an equivalent circuit model the BAW resonator is very similar to the crystal resonator.

The BAW resonator can be characterised by an equivalent Modified Butter-worth Van Dyke Model which is shown in fig 2.2

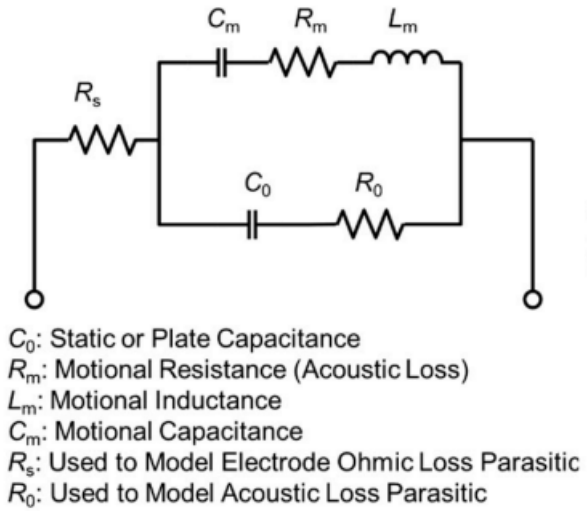

Figure 2.2: MBVD Model

Although this linear model is useful in modelling the resonator for most applications, it fails to capture any non linearities induced by the changes in DC bias. In order to combat these non-linearities Seungku Lee et al. [1] proposed a bias voltage dependent(V_{dc}) MBVD model as shown in Figure 2.3

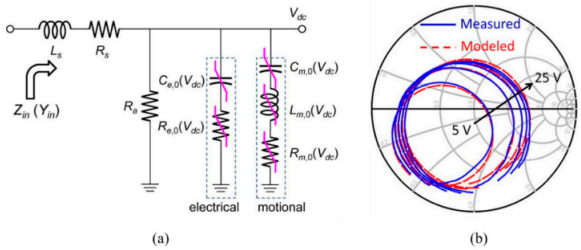

Figure 2.3: (a) Non-Linear MBVD Model. (b) Comparison between measured and modelled reflection parameters [1]

In terms of construction, these resonators can be broadly classified into two categories as shown in Figure 2.4

- FBAR(Thin Film Bulk Acoustic Resonator):The air gap increases quality factor as acoustic energy doesn't leak into substrate(Avago/Broadcom).
- Solidly Mounted Resonator(SMR): An acoustic reflector is placed under the bottom electrode and helps in reduction of energy loss through substrate(Qorvo).

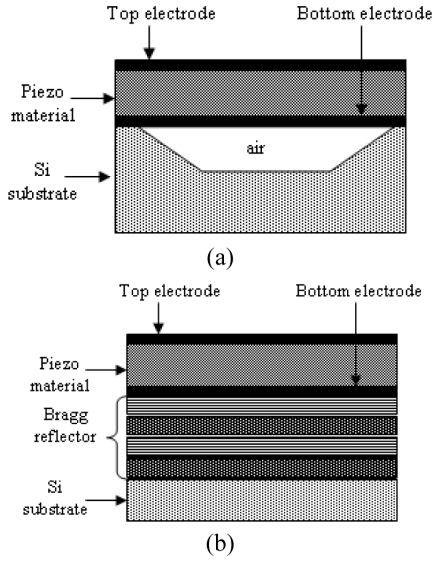

Figure 2.4: Types of BAW resonators: a)FBAR b) SMR [2]

2.1.2 ADVANTAGES OVER CRYSTALS

In order for BAW resonators to be an alternative to crystal resonators in clocking/timing applications,they must bring certain advantages to the table. The following few points highlight some such advantages.

- Due to the nature of construction of these devices, BAW resonators can be made smaller than the crystal counterparts. This leads to better integrated packaging which can lead to lower costs [17] as well better hardware security [18].

- Compared to crystal counterparts,BAW resonators offer better immunity to vibrations as seen in fig 2.5. This makes them more suitable for industrial, automotive and defense applications as these demand more robust system performance.

- BAW resonators can be constructed to resonate at much higher frequencies. Unlike crystal resonators which can be made to resonate in the order of few tens of Megahertz, BAW resonators can be designed to resonate at a few Gigahertz.

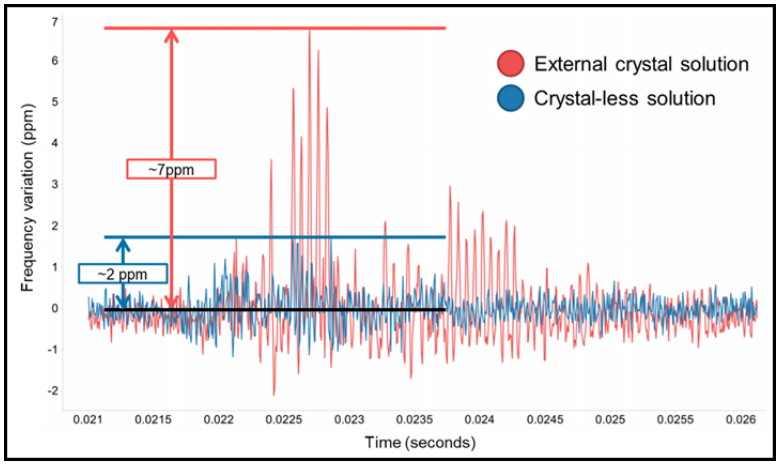

Figure 2.5: Crystal vs BAW vibration sensitivity

- A significant portion of the wake up time in wake up radio systems is wasted for the oscillator to startup and establish the system clock. BAW Oscillators have lower startup times compared to crystal counterparts.Lower startup times in oscillators gives power savings in duty cycled wireless communication (Figure 2.6) as the wake up time can be reduced in each cycle and hence the power savings add up to give a longer battery life.

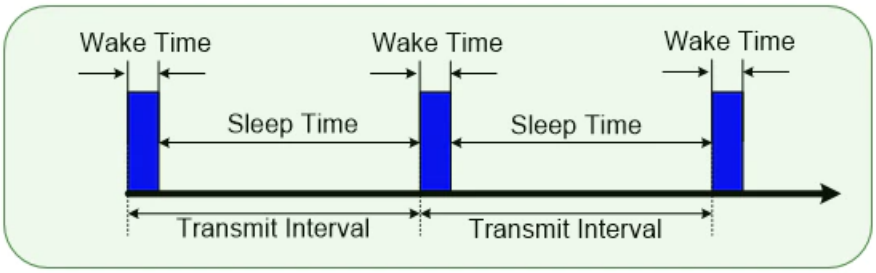

Figure 2.6: Wake up radio startup time

It should also be mentioned here that BAW resonators offer a much higher Q than integrated LC resonators. The caveat here is that the packaging parasitics have to be considered when the resonator is to be combined with active circuit elements on a separate silicon die.

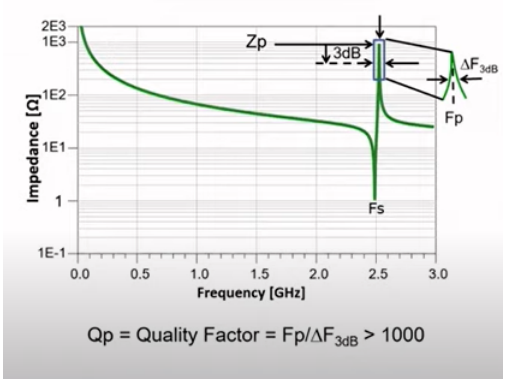

Figure 2.7: Resonator frequency plot

2.2 SINGLE ENDED OSCILLATOR TOPOLOGIES

The use of BAW resonators in oscillators has been explored slowly but steadily over the years. Although initially explored as a candidate for low phase noise oscillators, they demonstrate excellent Figure of merit for oscillators [19] and overcome limitations like limited tun-ability [20].

BAW oscillators have also been demonstrated to be a candidate for Wafer chip scale package(WCSP) integration [21]. Although the majority of oscillators use the resonator as parallel circuit element, there are instances when they have been designed using their series resonance [4] [22].

2.2.1 PIERCE ARCHITECTURE

In recent years one of the first oscillators that was designed using the BAW resonator as the tank element is presented in [3]. It can be seen in Fig 2.8, that the core device M_1 is responsible to set the trans-conductance Gm_1 in the loop gain equation given by

$$A_L = Gm_1.R_L.C_1/C_2$$

where R_L is the real part of the impedance seen at the drain node of M_1. It can be shown that a lower value of R_x results in a higher value of R_L by using the series to parallel transformation, given the Q of the resonator is high enough [23]. For optimal

stability and startup conditions, it is required that $C_1 = C_2$ which means that in order to minimize transconductance, the value of R_L has to be maximized.

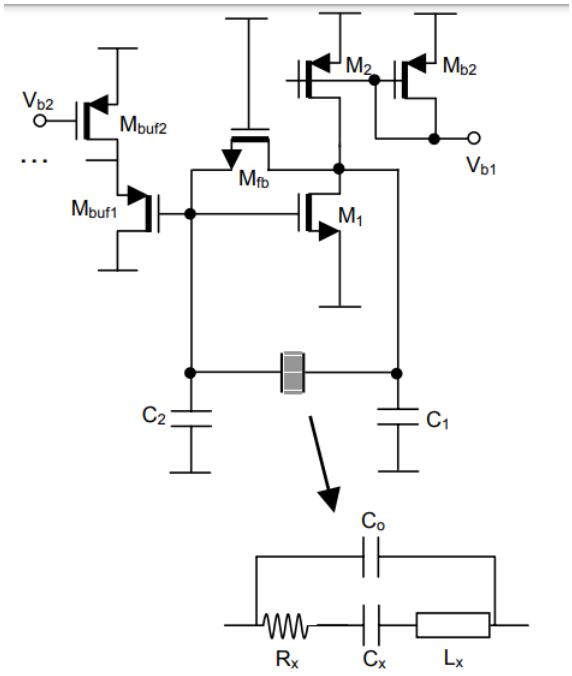

Figure 2.8: Pierce Oscillator using BAW resonator [3]

2.2.2 BUTLER ARCHITECTURE

Unlike the Pierce oscillator, the Butler architecture utilises the series resonance of the device [4]. In the schematic shown in fig 2.9,the transistor and the resistor were implemented in NXP's BiCMOS technology while the inductor and capacitors were integrated on a carrier substrate on which the BiCMOS die and the BAW die were flip chipped onto.

The drawback of using the Butler architecture is that the BAW resonator and the resonant frequency of the LC tank must be matched to within a few percent.

This oscillator circuit consumes 1.4mA of current from a 2.7V power supply and the resonator Q is 700 at 2GHz with passive temp compensation of 5ppm/C.The area occupied by the oscillator is 2.8 x 2.2 mm^2.A 6nH embedded inductor was also implemented on the laminate along with the flipped-chip active and BAW die.

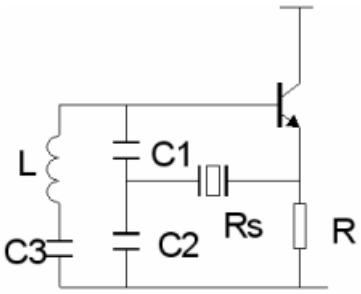

Figure 2.9: Butler Oscillator using BAW resonator [4]

2.2.3 COLPITT'S ARCHITECTURE

Another common single ended topology is the Colpitt's oscillator shown in Fig 2.10. The negative resistance is generated by using a BJT in the common collector topology and is given by

$$R_{neg} = \frac{g_m}{C_1.C_2.\omega^2}$$

Between f_s and f_p the BAW resonator acts like an inductor and this is used to create the oscillations by resonating it with the load capacticance C_L. The frequency of oscillation can be given by

$$f_{osc} = f_s \left(1 + \frac{C_m}{2(C_o + C_L)}\right)$$

where

$$C_L = \frac{(C_1 + C_\pi)C_2}{C_1 + C_\pi + C_2}$$

The phase noise of the oscillator can be minimised by increasing the amplitude of oscillation which can be accomplished by loweing the Value of C_2 capacitor.The caveat however is that higher oscillator amplitudes might lead to circuit instability.

For this oscillator [24],the quality factor of the resonator is about 600 with a resonant frequency of 2.1 Ghz with a 600ppm frequency variation. The active part of the circuit was implemented in 0.25um BiCMOS process.The oscillator circuit runs

off 2.5V power supply with a current consumption of 4.8mA

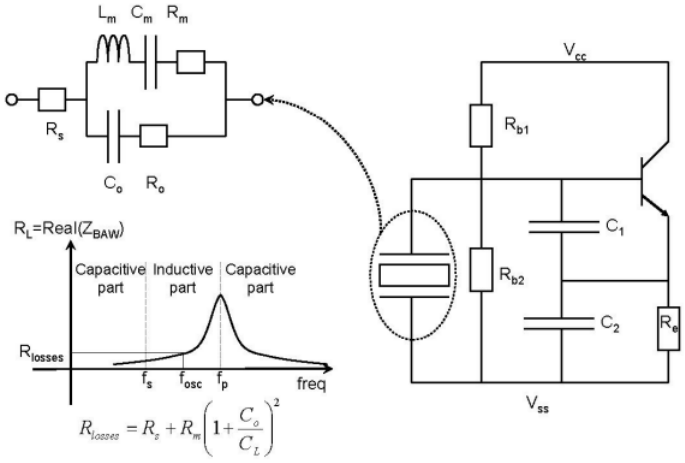

Figure 2.10: BAW based Colpitts Oscillator

2.3 DIFFERENTIAL OSCILLATOR TOPOLOGY

Although single ended topologies are easier to implement, differential topologies offer better supply rejection and common mode noise rejection. In this section we look at 3 common topologies of differential BAW oscillators

2.3.1 DIFFERENTIAL ARCHITECTURE

In case of a differential oscillator circuit,the active part of the circuit presents a negative resistance which is used to cancel the impedance presented by the BAW resonator at parallel resonance. The cross coupled pair presents a wideband negative resistance and hence is used as the core of the oscillator.However,because the DC impedance of the BAW resonator is different from that of an LC tank,additional circuit elements are needed to ensure proper operation.This architectural trade-offs will be described further in Chapter 4.

In [25],the authors used the cross coupled pair and created a BAW oscillator to be part of a QVCO.The frequency of operation of the oscillator is 2.1 GHz and it was shown that in 0.13um CMOS, it provided about 33dB of phase noise improvement over its integrated LC counterpart.

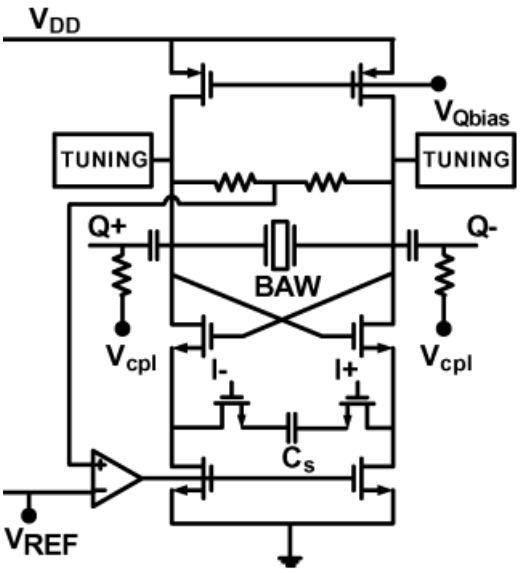

Figure 2.11: Differential BAW Oscillator

2.3.2 DIFFERENTIAL COLPITT'S

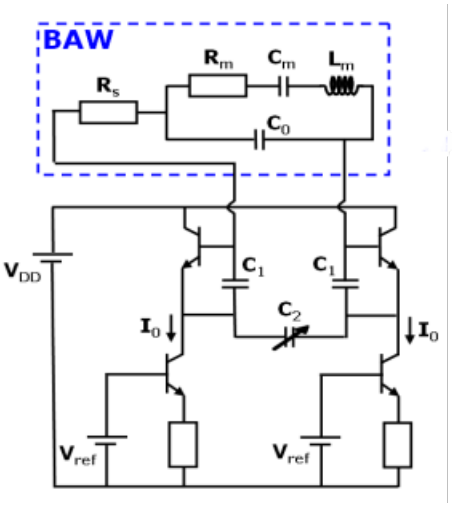

Figure 2.12: Differential Colpitts BAW Oscillator

Just like its single ended counterpart,the differential version of Colpitt's oscillator is quite popular in the RF applications as it provides good rejection against common mode noise. Fig 2.12 shows a differential Colpitt's [26], implemented in a 0.25um BiCMOS process. The ratio between C_1 and C_2 helps in setting the frequency of operation. The oscillator operates at 2.5GHz and consumes 10mA off a 2.7V supply.

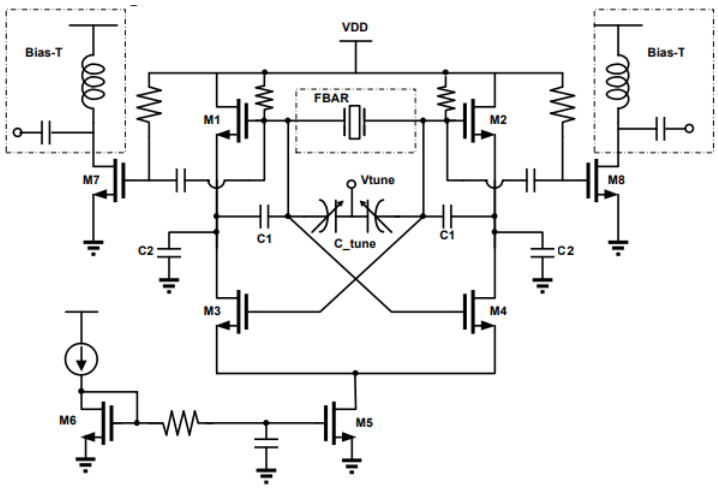

Figure 2.13: Gain boosted colpitts BAW Oscillator [5]

In case of the Colpitt's, gain boosting can be employed to improve startup requirements,increase the output swing and lower the phase noise. [5]

It can shown that the negative transconductance of the oscillator is increased by $1+(gm_3/gm_1).(1+C_1/C_2)$.This oscillator is useful in applications which have a lower supply voltage when compared to it's cross- coupled counterpart.

Another improvement that can be made to differential Colpitt's is to eliminate the tail current source by the use of a transformer and cross coupled capacitors [27]. This eliminates the 1/f noise contribution which results in reduction of close-in phase noise.

2.3.3 COMPLEMENTARY DIFFERENTIAL

The complementary cross coupled Fig 2.14 is the power efficient version of the cross coupled oscillator as it can reuse the bias current and this results in lower thermal noise. Compared to the 3 point oscillators described above,this architecture provides significant power savings for the same output amplitude.

In [28], the authors use this technique to demonstrate a 2.5 GHz Oscillator that consumes 675uW designed in 0.18um CMOS.

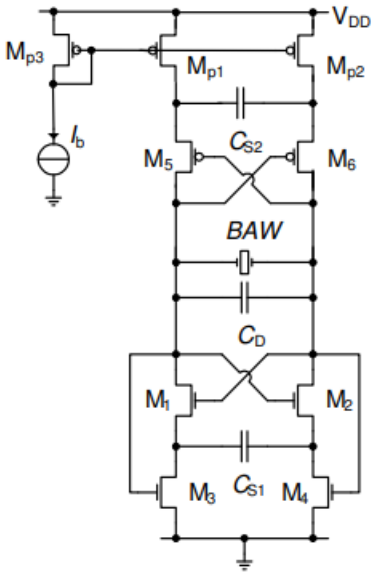

Figure 2.14: Complementary differential BAW

2.4 CHAPTER SUMMARY

In this chapter we introduced the BAW resonator and how it can be used to design oscillators. We also looked at various topologies of oscillators and in particular the cross coupled oscillator which will be used in our design due to its easier startup constraints.

CHAPTER 3: SUPER HARMONIC QUDRATURE VOLTAGE CONTROLLED OSCILLATORS

In chapter 1,we saw how different techniques like polyphase-phase filters, divide-by-two frequency dividers and quadrature voltage-controlled oscillators(QVCO) are different ways of generating Quadrature signals. Among these QVCOs offer better power and area efficiency as the frequencies go up.

QVCOs are created by using two identical oscillator cores and using a coupling network to create a phase relationship between the two cores. Based on the nature of the coupled signal, QVCOs can be classified into fundamental(first) mode or Super-harmonic(second) mode coupled oscillators.

Fundamental mode coupling often involves the use of active devices which can be used either in a parallel or series configuration.For the parallel version (PQVCO), four additional coupling transistors are added to the circuit which aid in coupling signals between the two oscillator cores [29].

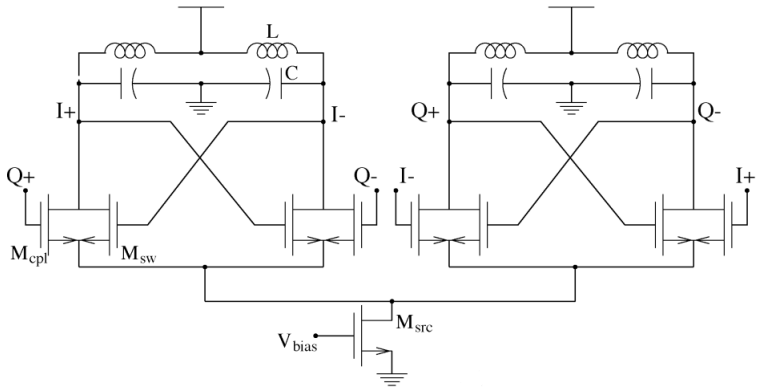

Figure 3.1: P-QVCO

It has been shown that there exists a trade off in the phase noise and the phase error in a PQVCO [30] [31]. Even within PQVCO,a disconnected source has a better phase

noise than the one where the sources are connected for the switching and coupling transistors [32].

In order to overcome the weak phase noise performance,two other coupling methods have been proposed in which the coupling transistors are added in series, either at top(TS-QVCO) of the switching transistors figure 3.2 or at the bottom of the switching transistors as shown in Figure 3.3

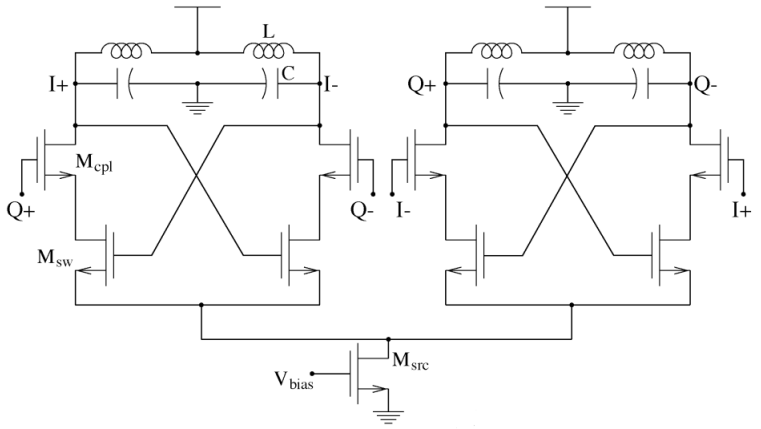

Figure 3.2: Top Series coupling-QVCO

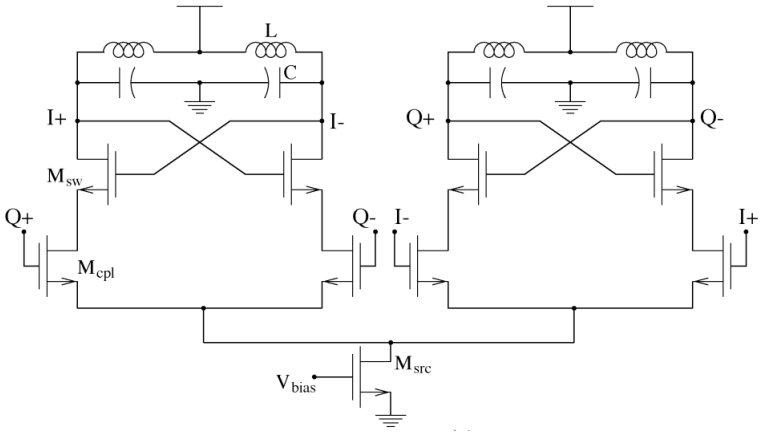

Figure 3.3: Bottom Series Coupling-QVCO

However in these cases, the oscillator is operated at a frequency that is slightly off from the resonant frequency of the tank circuit. This creates a reduction in the impedance seen looking into the tank as seen in figure 3.4

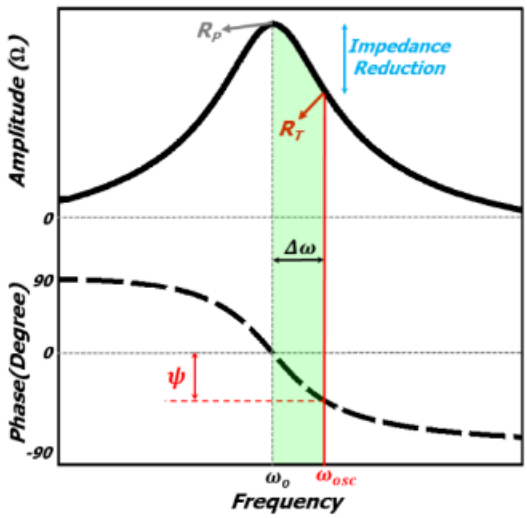

Figure 3.4: Impedance reduction

This phenomenon, which happens due to the phase difference between the oscillator core current and coupling currents,can be resolved by using the second harmonic of the oscillator instead of the fundamental as shown in fig.3.5

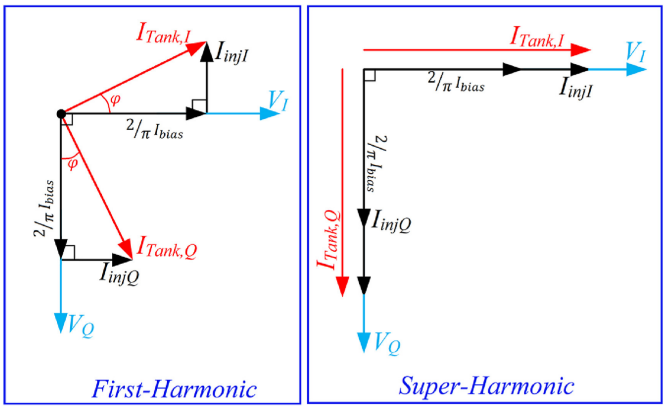

Figure 3.5: Tank voltage and current phasors in I and Q branches for fundamental and second harmonic coupling oscillators.

3.1 SUPER-HARMONIC COUPLING

The basic principle used in the Super-harmonic coupling is to use a network that will establish an anti-phase relationship between the second harmonic signals in two identical differential oscillators. This anti-phase relationship at the second harmonic translates to a quadrature lock in the fundamental. This is illustrated in figure

3.6.In the absence of the coupling network, the oscillators will be running freely and the phase difference between the two could be any arbitrary value. However as the coupling network is added, the common mode nodes are forced to run 180° out of phase by the network. This coupling happens at the second harmonic frequency of the oscillator output frequency.When the second harmonic is anti-phase, the fundamental locks into quadrature. This happens because the minima of the second harmonic aligns with the minima of the fundamental [33].

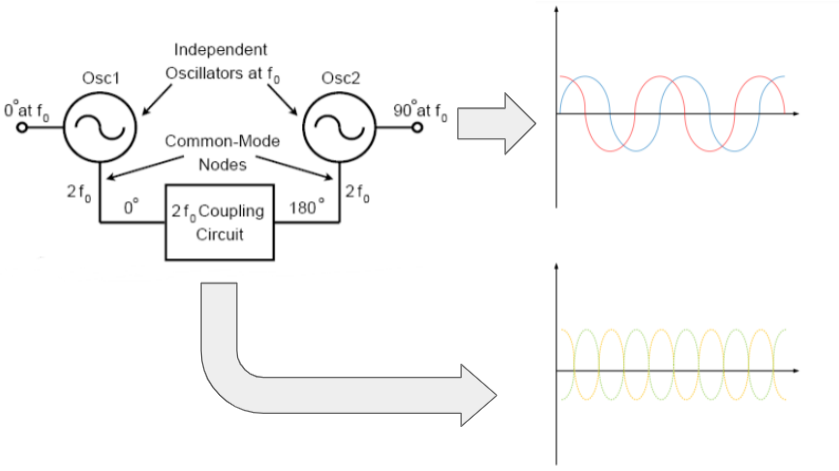

Figure 3.6: Super harmonic coupling principle.

It is a common technique to use the tail node of the differential pair as the coupling node in such oscillators as it creates a second harmonic signal without the use of additional circuitry. The second harmonic currents can be generated by using an auxiliary oscillator [34] or can be derived from the I and Q oscillators. [35] [36] [37]

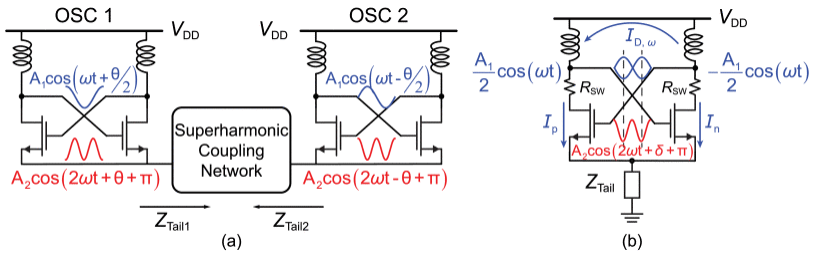

Figure 3.7: Super-Harmonic coupling using tail impedance engineering(a)Coupling architecture (b) corresponding half circuit [6]

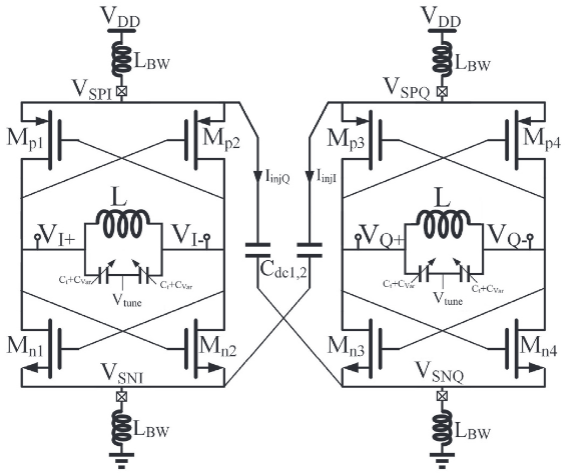

Figure 3.8: Current re-use Cross coupled Super harmonic Oscillator [7]

3.2 ACTIVE COUPLING

Super-harmonic coupling using active devices can be classified into two categories.

In the first category, the active circuitry is used to create another oscillator that operates at twice the frequency which is then used to inject the coupling currents into the I and Q oscillators [34]. The other method is to use an active device to modulate the impedance seen by the second harmonic signal such that it creates an anti-phase signal at the coupling nodes of the I and Q oscillators. [6] shows the use of such an active coupling network at the second harmonic to create a quadrature phase relationship. However in both of these methods, the use of active devices injects additional noise into the system which degrades the phase noise.

3.3 PASSIVE COUPLING

Among the passive methods of coupling, any network that can create an anti-phase relationship at the second harmonic between the I and Q cores, can give rise to a quadrature lock at the fundamental frequency.

[38] uses a transformer to couple the common mode second harmonic signals that are tapped from the tail node of the differential switching pair. The fact that it is passive and uses super-harmonic coupling makes it appealing for better phase noise

performance. The drawback of this approach is the large die area required for the layout of the transformer.

[7] show the use of a passive coupling network to achieve quadrature oscillations in a current re-use cross coupled CMOS oscillator.

Besides these methods, some other passive methods of super-harmonic coupling are capacitive coupling the common mode signal in to the tail current [36],using the tuning cap as coupling node [37] and AC shorting the tail current nodes [9].

3.4 CHAPTER SUMMARY

In this chapter we described the process of super-harmonic coupling along with some methods by which to generate this coupling. The objective of this chapter was to prepare the reader for the coupling technique introduced in this thesis which is a passive super-harmonic coupling method.

CHAPTER 4: A NOVEL BULK ACOUSTIC WAVE BASED SUPER-HARMONIC QUADRATURE VOLTAGE CONTROL OSCILLATOR

As mentioned in the first chapter,there are several ways to generate quadrature signals. Among the coupling methods,the two most used are the fundamental mode(first harmonic) or super harmonic(second harmonic) coupling methods.These methods also can be further classified into active and passive modes of coupling which have their advantages/disadvantages. In terms of published designs, the only quadrature VCO using a BAW device uses fundamental mode coupling. Although the design uses the BAW resonators to achieve low phase noise and power consumption, coupling using fundamental mode has two disadvantages.

- The additional coupling transistors add extra noise to the circuit
- The off resonance operation of the tank further keeps it away from maximum achievable phase noise performance.

In this chapter we introduce the basic cross coupled BAW oscillator, the equivalent small circuit model of the oscillator and finally the quadrature VCO architecture using this BAW oscillator.

As stated above, this oscillator uses no extra active devices for achieving quadrature lock and also the tank circuit(described in the small signal model) is able to operate at resonance, both of which help in achieving lower phase noise.

4.1 THE BASIC CROSS COUPLED BAW OSCILLATOR

The BAW cross coupled oscillator is very similar to the LC tank cross oscillator. The BAW resonator itself can be considered as an inductor near its parallel resonant

frequency, for the purposes of comparison between the two. The tank is completed with the addition of a tun-able capacitor.

A cross coupled transistor pair drives the tank differentialy in order to excite its parallel resonance, thereby acting as a negative parallel resistor, to supply the energy lost in a cycle of oscillation, back to the tank.

Despite the similarities BAW based oscillators have two major differences from their LC counterparts.

- To prevent de-tuning the BAW resonator at high frequencies,a high impedance load is used to bias the structure. In the case of the LC oscillators, the same tank inductor could be used to provide the bias voltage. The usage of a fully differential structure to bias the oscillator means that the common mode of the oscillator has to set by using feedback.

- The resonator provides a high impedance at low frequencies. So if the cross coupled pair provides a negative resistance across all frequencies, the circuit would end up latching. In order to prevent this from happening, it is required to incorporate a high pass response into the negative resistance. This can be achieved by adding a degenerative capacitor at the source node which reduces the negative resistance at low frequencies and yet creating a short at high frequencies.

Keeping these differences in mind, the basic BAW oscillator shown in the figure is chosen the building block of the oscillator. As it can be seen the circuit is fully differential biased with current mirrors and uses Common mode feedback for setting the operating point. It also uses a degenerative capacitor to prevent it from latching.

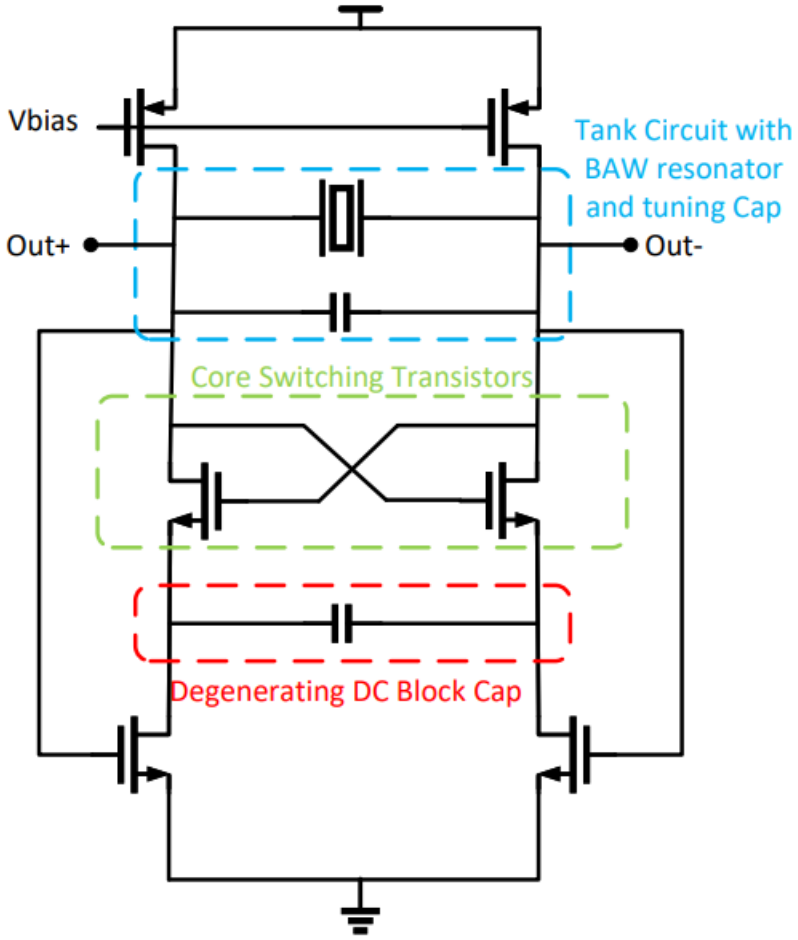

Figure 4.1: BAW Oscillator

4.2 SMALL SIGNAL LINEAR MODEL

Before we look at the proposed architecture, it is important to break down the basic BAW oscillator and look at the small signal linear model.

As seen in the figure, the oscillator small signal model consists of three different parts.

- The resonator
- The tuning cap
- The active circuit

The resonator is represented by the equivalent Butterworth-Van Dyke model. The circuit can be simplified to an equivalent Inductor given by Lm at the parallel resonant frequency. The equivalent capacitance for the tank can be approximately given by

$$C_{tank} = C_e + C_t + C_{osc}$$

where the 3 terms represents the electrode capacitance of the resonator, the tuning capacitance and the parasitic capacitance of the active circuit respectively.

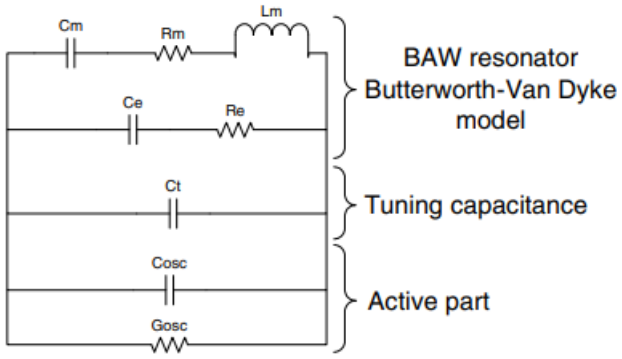

Figure 4.2: Small signal Linear model of the Oscillator

It can be further shown that the net impedance of the active part of the small circuit can be given by

$$G_{osc} = \frac{-2}{g_m}[1 + \frac{g_m}{2sC_s}]$$

where C_s is the capacitance coupling the two source nodes.The equivalent negative resistance at high frequencies is $-2/g_m$. The choice of this capacitor is critical as it sets the negative resistance pole frequency and reducing it will reduce the loop gain at the parallel resonant frequency. However setting C_s too high is also an issue as the cross coupled pair looks inductive when it is degenerated by a capacitor and this inductance could potentially resonate with the plate capacitance of the BAW.

4.3 PROPOSED QUADRATURE SUPER-HARMONIC COUPLING QVCO

As it was seen previously the degenerative capacitor plays an important role in the stability of the circuit and the presence of this component in the circuit was therefore exploited to propose a new coupling mechanism that leverages the circuit symmetry to achieve super-harmonic coupling using passive elements to give rise to a novel QVCO architecture.

Using the principal of symmetry in a differential structure, the capacitor C_s could be in theory split into two series capacitors of double the value. In doing so,we create a node of symmetry in the circuit where the odd modes cancel but the even modes add constructively. If we create two instances of this base oscillator we can ensure a 180 phase difference of the even mode by connecting a passive element(an inductor) across the two corresponding nodes.

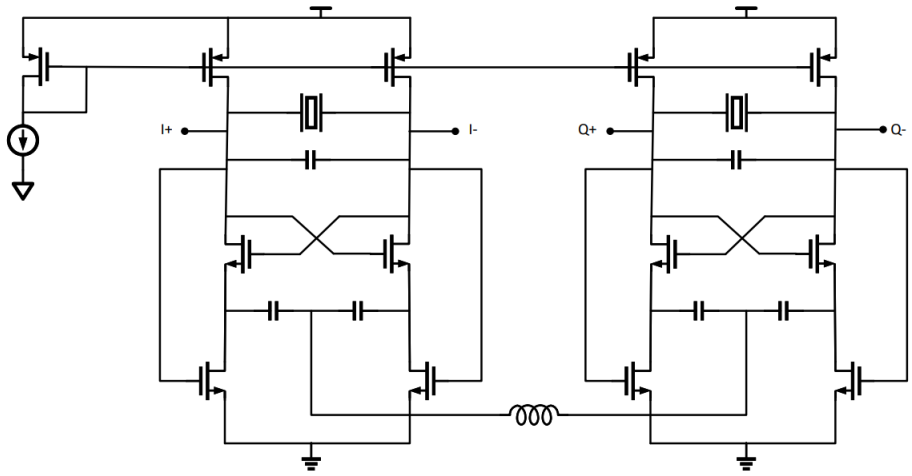

Figure 4.3: Superharmonic BAW QVCO

It will be shown in the later section that if the second harmonic is forced into a 180° phase difference, the fundamental modes oscillate at a 90° phase difference.

4.4 PHASE RELATIONSHIP BASED ON SECOND HARMONIC CURRENTS

For evaluating the current through each transistor is a function of the DC overdrive voltage

and the instantaneous AC voltages at the Gate and Source

The DC overdrive can be written as

$$V_{OV} = V_G - V_S - V_t \tag{4.1}$$

where

The current through the 4 transistors can be modelled as

$$I_{DI1} = K[V_{OV} + A_1 cos(\omega t) - A_2 cos(2\omega t + \pi)]^2 \tag{4.2}$$

$$I_{DI2} = K[V_{OV} + A_1 cos(\omega t + \pi) - A_2 cos(2\omega t + \pi)]^2 \tag{4.3}$$

$$I_{DQ1} = K[V_{OV} + A_1 cos(\omega t + \theta) - A_2 cos(2\omega t + \pi + 2\theta)]^2 \tag{4.4}$$

$$I_{DQ2} = K[V_{OV} + A_1 cos(\omega t + \pi + \theta) - A_2 cos(2\omega t + \pi + 2\theta)]^2 \tag{4.5}$$

where

A_1=Fundamental Amplitude at Output

A_2=Second harmonic amplitude at Common Source node

K=Transistor parameter

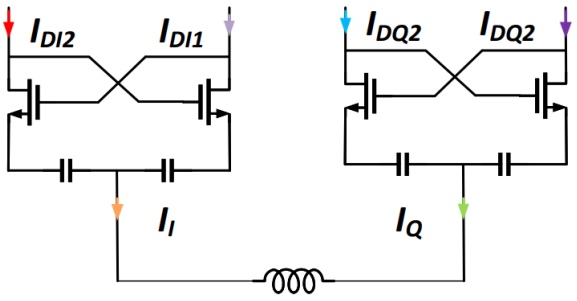

Figure 4.4: Currents in the Oscillator core

Expanding the expressions,

$$I_{DI1} = K[V_{OV}^2 + A_1^2 cos^2(\omega t) + A_2^2 cos^2(2\omega t + \pi) + 2.V_{OV}.A_1 cos(\omega t) \\ -2.V_{OV}.A_2.cos(2\omega t + \pi) - 2.A_1.A_2.cos(\omega t).cos(2\omega t + \pi)] \tag{4.6}$$

$$I_{DI2} = K[V_{OV}^2 + A_1^2 cos^2(\omega t + \pi) + A_2^2 cos^2(2\omega t + \pi) + 2.V_{OV}.A_1 cos(\omega t + \pi) \\ -2.V_{OV}.A_2.cos(2\omega t + \pi) - 2.A_1.A_2.cos(\omega t + \pi).cos(2\omega t + \pi)] \tag{4.7}$$

$$I_{DQ1} = K[V_{OV}^2 + A_1^2 cos^2(\omega t + \theta) + A_2^2 cos^2(2\omega t + \pi + 2\theta) + 2.V_{OV}.A_1 cos(\omega t + \theta) \\ -2.V_{OV}.A_2.cos(2\omega t + \pi + 2\theta) - 2.A_1.A_2.cos(\omega t + \theta).cos(2\omega t + \pi + 2\theta)] \tag{4.8}$$

$$I_{DQ2} = K[V_{OV}^2 + A_1^2 cos^2(\omega t + \pi + \theta) + A_2^2 cos^2(2\omega t + \pi + 2\theta) + 2.V_{OV}.A_1 cos(\omega t + \pi + \theta) \\ -2.V_{OV}.A_2.cos(2\omega t + \pi + 2\theta) - 2.A_1.A_2.cos(\omega t + \pi + \theta).cos(2\omega t + \pi)] \tag{4.9}$$

Simplifying the expressions to isolate harmonic components

$$\begin{aligned} I_{DI1} = K[V_{OV}^2 + \frac{1}{2}(A_1^2 + A_2^2) + \frac{1}{2}A_1^2 cos(2\omega t) + \frac{1}{2}A_2^2 cos(4\omega t) \\ +2.V_{OV}.A_1 cos(\omega t) - 2.\frac{1}{2}.A_1.A_2.(cos(\omega t + \pi) + cos(3\omega t + \pi)) \\ -2.V_{OV}.A_2 cos(2\omega t + \pi)] \end{aligned} \tag{4.10}$$

$$\begin{aligned} I_{DI2} = K[V_{OV}^2 + \frac{1}{2}(A_1^2 + A_2^2) + \frac{1}{2}A_1^2 cos(2\omega t) + \frac{1}{2}A_2^2 cos(4\omega t) \\ +2.V_{OV}.A_1 cos(\omega t + \pi) - 2.\frac{1}{2}.A_1.A_2.(cos(\omega t) + cos(3\omega t + 2\pi)) \\ -2.V_{OV}.A_2 cos(2\omega t + \pi)] \end{aligned} \tag{4.11}$$

$$\begin{aligned} I_{DQ1} = K[V_{OV}^2 + \frac{1}{2}(A_1^2 + A_2^2) + \frac{1}{2}A_1^2 cos(2\omega t + 2\theta) + \frac{1}{2}A_2^2 cos(4\omega t + 4\theta) \\ +2.V_{OV}.A_1 cos(\omega t + \theta) - 2.\frac{1}{2}.A_1.A_2.(cos(\omega t + \pi + \theta) + cos(3\omega t + \pi + 3\theta)) \\ -2.V_{OV}.A_2 cos(2\omega t + \pi + 2\theta)] \end{aligned} \tag{4.12}$$

$$\begin{aligned} I_{DQ2} = K[V_{OV}^2 + \frac{1}{2}(A_1^2 + A_2^2) + \frac{1}{2}A_1^2 cos(2\omega t + 2\theta) + \frac{1}{2}A_2^2 cos(4\omega t + 4\theta) \\ +2.V_{OV}.A_1 cos(\omega t + \pi + \theta) - 2.\frac{1}{2}.A_1.A_2.(cos(\omega t + \theta) + cos(3\omega t + 2\pi + 3\theta)) \\ -2.V_{OV}.A_2 cos(2\omega t + \pi + 2\theta)] \end{aligned} \tag{4.13}$$

The DC blocking capacitors in the source will block the DC components.Also the odd harmonic terms cancel each other.

$$\begin{aligned} I_I &= I_{DI1} + I_{DI2} \\ &= K[A_1^2 cos(2\omega t) + A_2^2 cos(4\omega t) - 4.V_{OV}.A_2 cos(2\omega t + \pi)] \end{aligned} \tag{4.14}$$

$$\begin{aligned} I_Q &= I_{DQ1} + I_{DQ2} \\ &= K[A_1^2 cos(2\omega t + 2\theta) + A_2^2 cos(4\omega t + 4\theta) - 4.V_{OV}.A_2 cos(2\omega t + \pi + 2\theta)] \end{aligned} \tag{4.15}$$

Using KCL

$$I_I + I_Q = 0 \tag{4.16}$$

$$\begin{aligned} \implies K[A_1^2 cos(2\omega t) + A_2^2 cos(4\omega t) - 4.V_{OV}.A_2 cos(2\omega t + \pi)] + \\ K[A_1^2 cos(2\omega t + 2\theta) + A_2^2 cos(4\omega t + 4\theta) - \\ 4.V_{OV}.A_2 cos(2\omega t + \pi + 2\theta)] = 0 \end{aligned} \tag{4.17}$$

The Fourth harmonic current will be attenuated by the inductor and we are left the following terms

$$\begin{aligned} K[A_1^2 cos(2\omega t) - 4.V_{OV}.A_2 cos(2\omega t + \pi)] + \\ K[A_1^2 cos(2\omega t + 2\theta) - 4.V_{OV}.A_2 cos(2\omega t + \pi + 2\theta)] = 0 \end{aligned} \tag{4.18}$$

For non-zero values of K, A_1, V_OV and A_2,the solution of the equation above becomes

$$\theta = (2n + 1)\pi/2 \tag{4.19}$$

where n is an integer.

Since the period of the signals is 2π,the phase relationship between I and Q channels will be $+\pi/2$ or $-\pi/2$.

4.5 CHAPTER SUMMARY

In this chapter we introduced the novel super-harmonic coupled BAW based quadrature voltage controlled oscillator. We described the basic cross coupled oscillator and presented the analytical model of how the coupling creates the quadrature relationship in the I and Q oscillators. In the next chapter we demonstrate the the performance of the circuit using simulations and compare it to its fundamental mode coupling equivalent.

CHAPTER 5: SIMULATION RESULTS

5.1 CIRCUIT IMPLEMENTATION

In order to verify the proposed concept, the oscillator was designed in two processes. In the first design, the QVCO was designed in a 0.13um 6-metal FD-SOI process. The BAW resonator was modelled by using measured s-parameter data from an available source. The center frequency of the resonator was 5.8 GHz.

5.2 PHASE NOISE COMPARISON

5.2.1 GPDK IMPLEMENTATION

For the phase noise comparision, the propsed QVCO was implemented in a 45nm GPDK from NCSU. The supply voltage was chosen to be 1V and the switching transistors(NMOS) were sized at 50um/45nm while the PMOS Load transistors were sized at 50um/1um. This was because the NMOS switching transistors were deigned for fastest switching times with enough current density whereas the width of the PMOS transistors were designed for carrying enough current but longer length made sure we were presenting a high impedance to the switching nodes.

Additionally the NMOS tranistors used in the tail current sources were sized at 50um/10um.The tail coupling capacitor was set to 250fF on each side(differentially) whereas the inductor was chosen to be 2nH.

The entire circuit consumes 1mW of power accounting for all the bias branches while working of a 1V supply.

5.2.2 COMPARISON WITH FUNDAMENTAL MODE OPERATION

In order to establish the improvement in phase noise due to the use of this technique, it was essential to compare the super-harmonic QVCO to a fundamental mode QVCO.

This comparison had to be between two oscillators with identical parameters. By adding parallel coupling transistor and removing the coupling inductors, the proposed QVCO was modified into the BAW based parallel QVCO as shown in Figure 5.1

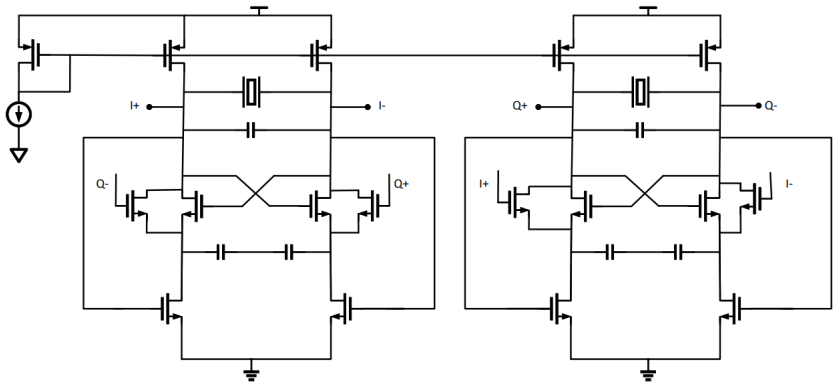

Figure 5.1: BAW based Parallel coupling QVCO

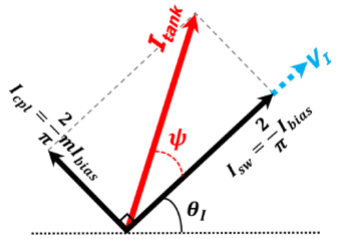

Figure 5.2: Phasor Diagram for tank current in Parallel coupling QVCO

$$\psi = \tan^{-1}(I_{cpl}/I_{sw}) = \tan^{-1}(W_{cpl}/W_{sw}) = \tan^{-1}(m)$$

Also for a second order RLC network, the phase deviation from resonace can be expressed as

$$\tan\psi = \frac{2Q(\omega_{osc} - \omega o)}{\omega_o} = \frac{2Q\Delta\omega}{\omega_o}$$

where Q is the quality factor of the tank circuit.

From these two equations we can calculate the frequency of oscillation as the following.

$$\omega_{osc} = \omega_o(1 + \frac{m}{2Q})$$

This deviation in the frequency of operation results in the degradation of phase noise. At the same time, the frequency of operation in case of super-harmonic coupling is the same as the resonant frequency of the tank.

It can be seen from the table that if all things are kept constant, this method of coupling, the phase noise of the oscillator using fundamental mode coupling is higher.

Table 5.1: Comparison of SH and Fundamental mode Oscillators

	Super-harmonic QVCO	Fundamental Coupled QVCO
Supply Voltage(V)	1	1
Current consumption(A)	1m	1m
Frequency of Operation(Hz)	5.8G	5.8G
Phase Noise @ 1 MHz offset(dBc/Hz)	-136.9	-132.8

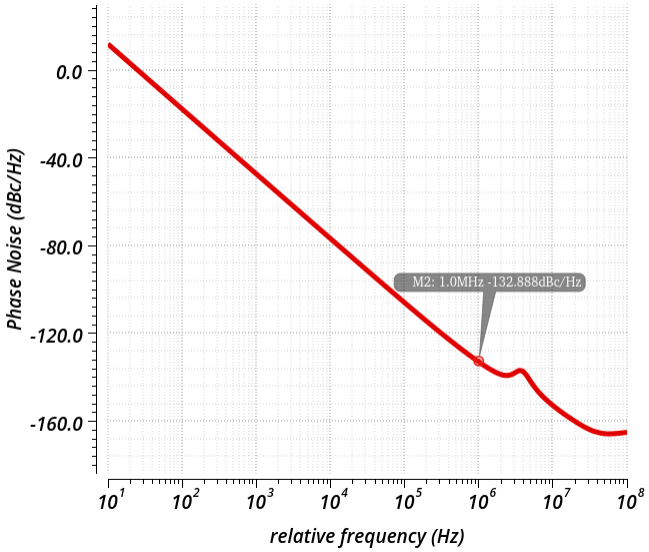

Figure 5.3: Phase Noise @ 1M Fund

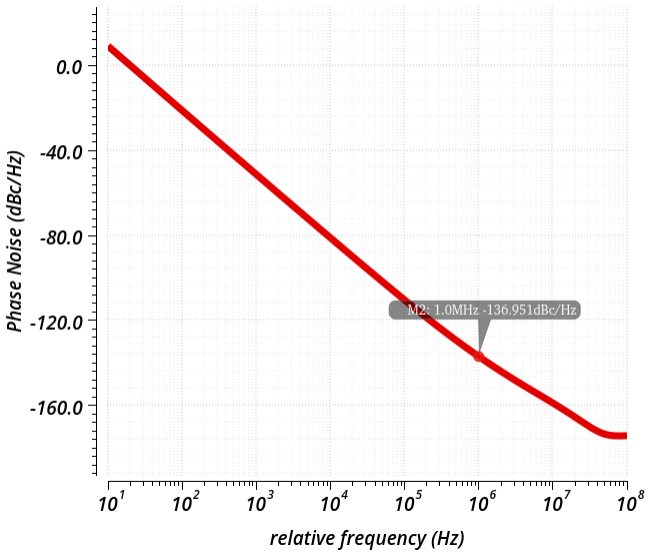

Figure 5.4: Phase Noise @ 1M SH

5.3 TIME DOMAIN STABLITY

5.3.1 FD SOI IMPLEMENTATION

The same ciruit was implemented using components from the Global Foundries FD S0I process. The supply voltage was chosen to be 1.5V and the switching transistors(NMOS) were sized at 30um/90nm while the PMOS Load transistors were sized at 50um/1um. Additionally the NMOS tranistors used in the tail current sources were sized at 50um/10um. The tail coupling capacitor was set to 200fF on each side(differentially) whereas the inductor was chosen to be 2nH.

5.3.2 STABILITY VERIFICATION USING PULSE INJECTION

Ir order to verify the phase stability of the structure, time domain simulation was used. As the two oscillator cores started, it was observed that the startup time in both was different. After the Oscillators reached steady state,the positive output of the I side was shorted with the positive output of the Q side, whereas the negative outputs were shorted together. The whole time domain settling of the second harmonic signal with respect to the phase reset and injected current pulse can be seen in Figure 5.5

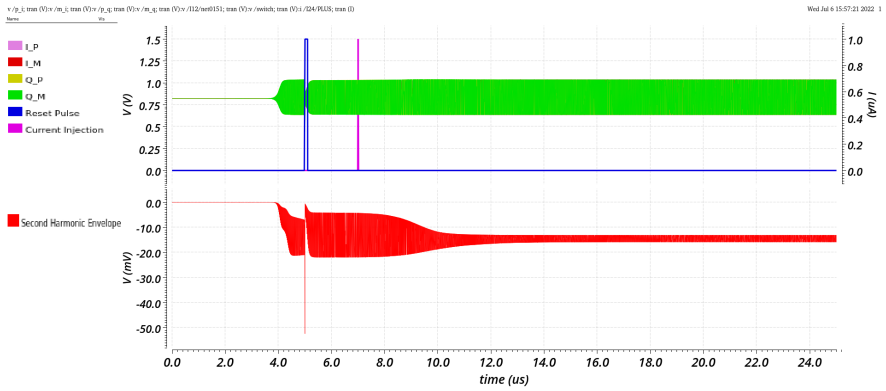

Figure 5.5: Summary:Phase reset and pulse injection

It can be seen from Figure 5.6 that after the phase reset,the amplitude of oscillation gets restored within 0.5us and so does the second harmonic envelope.

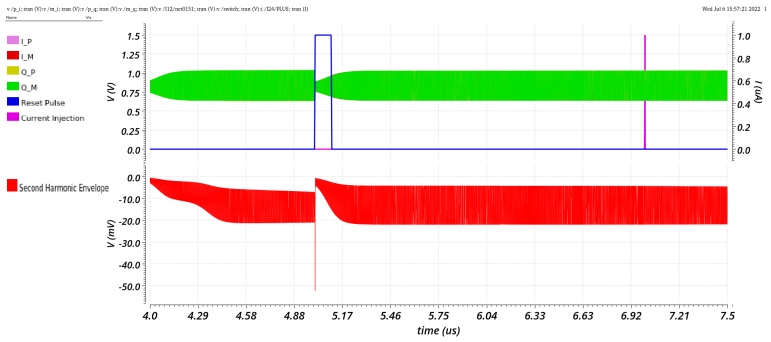

Figure 5.6: Second harmonic envelope during phase reset

After the phase reset period is over, the oscillator is allowed to run for another 2us. At this instant, a current pulse of 1uA is injected into the I side tank for a duration of 10ps.

As it can be seen from Figure 5.7, the phase of the I and Q channels stays the same and doesn't abruptly change. This ensures that the amount of charge injected into the tank was low enough to not affect the phase of the output wave-forms.

At the end of 24 us, it can be seen in Figure 5.8that the phase has locked in quadrature with the second harmonic envelope being very stable.

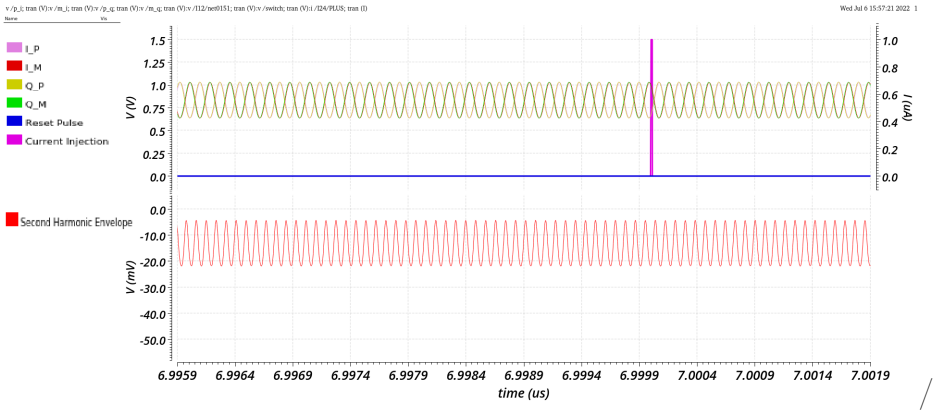

Figure 5.7: Inject pulse:Phase stays constant

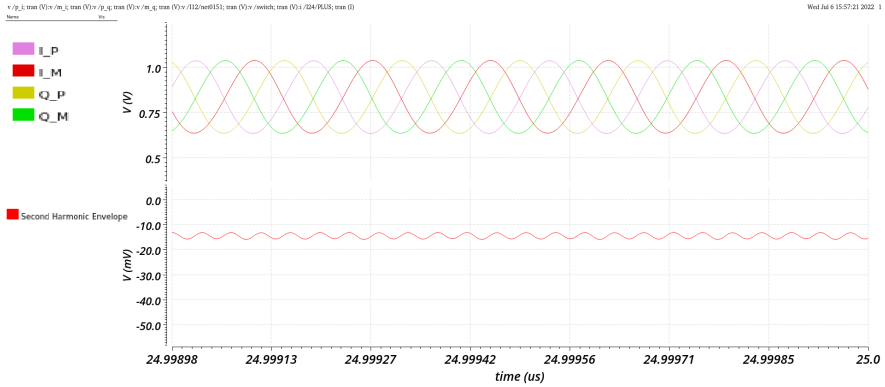

Figure 5.8: Quadrature phase established after pulse injection

5.4 CONCLUDING REMARKS

In this chapter we demonstrated the improvements in phase noise that using Superharmonic coupling provides when compared to fundamental mode coupling when applied to generate quadrature signals using the same oscillator core. We also demonstrated the stability of the quadrature mode when it was perturbed after startup.

CHAPTER 6: CONCLUSION

This thesis describes a novel Bulk Acoustic Wave based Super-harmonic Quadrature Voltage Controlled Oscillator.We began by introducing the role of Quadrature VCOs in signal processing and followed it up with comparisons with various methods to generate quadrature signals. Next we discussed how BAW based oscillators are designed and looked at various topologies that have been designed in the past. We then presented the oscillator circuit,which is the novel contribution of this work,along with an analysis of how it works to achieve quadrature lock. The circuit was implemented in two technologies and the results of the simulations were also presented in order to demonstrate the working principle.

6.1 COMPARISON WITH OTHER QVCO

Although this is the first superharmonically coupled BAW QVCO as per our knowledge,it was important to compare the performace of the QVCO to the only other BAW based QVCO known in the literature.The results of the comparision are summarised in table 6.1

The Figure Of Merit(FOM) of the oscillator was computed as per the formula shown below.

$$FOM = 20log\frac{\omega_o}{\Delta\omega} - L(\Delta\omega) - 10log(P_{DC}(mW))$$

Table 6.1: Performance Summary and Comparison of QVCO with similar work

	Power Consumption (mW)	Frequency (GHz)	Phase Noise (dBc/Hz) @1 MHz offset	FOM(dB)	Coupling method	Resonator type	CMOS Technology (um)
Ng [39]	**5**	**17**	**-110**	**187.6**	**Fundamental**	**LC**	**0.18**
Yao [40]	**27.7**	**5.1**	**-132.6**	**192**	**Super-harmonic**	**LC**	**0.18**
Kim [41]	**5.4**	**1.1**	**-120**	**173.5**	**Fundamental**	**LC**	**0.18**
Rai [25]	**0.6**	**2.1**	**-143.5**	**212.1**	**Fundamental**	**BAW**	**0.13**
This work	**1**	**5.8**	**-136.9**	**212.1**	**Super-Harmonic**	**BAW**	**0.045**

6.2 FUTURE WORK

The list of future tasks that can be supplemented to this work can be identified as follows

- Tape-out of oscillator: This will include laying out of the circuit and adding additional buffer/test circuit to aid in measurements
- High Frequency FOM:It can be explored to see whether a higher frequency resonator will aid in a better FOM.
- Test circuits:A Mixer and some baseband circuity can be added to verify phase accuray of the QVCO
- Modelling of Packaging losses:In order for the system to work,the resonator and the CMOS die have to be put on a laminate.The design of the Laminate will include minimzing losses incured during going from one die to another

REFERENCES

[1] S. Lee, V. Lee, S. A. Sis, and A. Mortazawi, "Large-signal performance and modeling of intrinsically switchable ferroelectric FBARs," *IEEE Transactions on Microwave Theory and Techniques*, vol. 61, pp. 415–422, jan 2013.

[2] M. Li, S. Seok, N. Rolland, P. A. Rolland, H. E. Aabbaoui, E. D. Foucauld, P. Vincent, and V. Giordano, "Ultralow-phase-noise oscillators based on BAW resonators," *IEEE Transactions on Ultrasonics, Ferroelectrics, and Frequency Control*, vol. 61, pp. 903–912, jun 2014.

[3] B. Otis and J. Rabaey, "A 300mw 1.9-GHz CMOS oscillator utilizing micromachined resonators," *IEEE Journal of Solid-State Circuits*, vol. 38, pp. 1271–1274, jul 2003.

[4] F. Vanhelmont, P. Philippe, A. B. M. Jansman, R. F. Milsom, J. J. M. Ruigrok, and A. Oruk, "A 2 GHz reference oscillator incorporating a temperature compensated BAW resonator," in *2006 IEEE Ultrasonics Symposium*, IEEE, 2006.

[5] J. Shi and B. P. Otis, "A sub-100uw 2GHz differential colpitts CMOS/FBAR VCO," in *2011 IEEE Custom Integrated Circuits Conference (CICC)*, IEEE, sep 2011.

[6] L. Zhang, N.-C. Kuo, and A. M. Niknejad, "A 37.5–45 GHz superharmonic-coupled QVCO with tunable phase accuracy in 28 nm CMOS," *IEEE Journal of Solid-State Circuits*, vol. 54, pp. 2754–2764, oct 2019.

[7] J. Mazloum and S. Sheikhaei, "C3S-QVCO: A low phase noise low power superharmonic coupling qvco with cross-connected common-source nodes," *Microelectronics Journal*, vol. 107, p. 104944, 2021.

[8] F. E. Idachaba and H. Orovwode, "Analysis of a Weaver, Hartley and Saw-Filter Based, Image Reject Architectures for Radio Receiver Design," *Advanced Materials Research*, vol. 367, pp. 199–204, oct 2011.

[9] B. Soltanian and P. Kinget, "A low phase noise quadrature LC VCO using capacitive common-source coupling," in *2006 Proceedings of the 32nd European Solid-State Circuits Conference*, IEEE, sep 2006.

[10] J. Cabanillas, L. Dussopt, J. Lopez-Villegas, and G. Rebeiz, "A 900 MHz low phase noise CMOS quadrature oscillator," in *2002 IEEE Radio Frequency Integrated Circuits (RFIC) Symposium. Digest of Papers (Cat. No.02CH37280)*, IEEE.

[11] O. Esmaeeli, B. Jafari, and S. Sheikhaei, "A super-harmonic coupling QVCO using a frequency doubler circuit," in *Electrical Engineering (ICEE), Iranian Conference on*, IEEE, may 2018.

[12] A. Schaer, "Behavior and current performances of SAW and BAW oscillators," in *1976 6th European Microwave Conference*, IEEE, sep 1976.

[13] F. Bi and B. Barber, "Bulk acoustic wave RF technology," *IEEE Microwave Magazine*, vol. 9, pp. 65–80, oct 2008.

[14] K.-y. Hashimoto, *RF Bulk acoustic wave filters for communications*. Artech House, 2009.

[15] K. Lakin, J. Belsick, J. McDonald, and K. McCarron, "Improved bulk wave resonator coupling coefficient for wide bandwidth filters," in *2001 IEEE Ultrasonics Symposium. Proceedings. An International Symposium (Cat. No.01CH37263)*, IEEE.

[16] G. G. Fattinger, "BAW resonator design considerations - an overview," in *2008 IEEE International Frequency Control Symposium*, IEEE, may 2008.

[17] E. Marigo, M. Soundara-Pandian, J. Bin, J. Din, N. S. B. Roslan, A. Fawzy, A. Yasser, M. Atef, and A. Ahmed, "Monolithic BAW oscillator with conventional QFN packaging," in *2019 Joint Conference of the IEEE International Frequency Control Symposium and European Frequency and Time Forum (EFTF/IFC)*, IEEE, apr 2019.

[18] S. Shahraini, H. Luo, T. Huusari, E. Alban, S. Kundu, R. Jain, J. Mix, B. Carlton, R. Abdolvand, M. Abdelmoneum, and N. Kurd, "Resilient ultra stable CMOS-MEMS oscillator with receiver in intel 22FFL technology," in *2021 IEEE 34th International Conference on Micro Electro Mechanical Systems (MEMS)*, IEEE, jan 2021.

[19] A. Nelson, J. Hu, J. Kaitila, R. Ruby, and B. Otis, "A 22uW, 2.0 GHz FBAR oscillator," in *2011 IEEE Radio Frequency Integrated Circuits Symposium*, IEEE, jun 2011.

[20] P. Guillot, P. Philippe, C. Berland, and J.-F. Bercher, "A 2GHz 65nm CMOS digitally-tuned BAW oscillator," in *2008 15th IEEE International Conference on Electronics, Circuits and Systems*, IEEE, aug 2008.

[21] B. Bahr, A. Kiaei, M. Chowdhury, B. Cook, S. Sankaran, and B. Haroun, "Near-field-coupled bondless BAW oscillators in WCSP package with 46fs jitter," in *2021 IEEE Radio Frequency Integrated Circuits Symposium (RFIC)*, IEEE, jun 2021.

[22] J. Hu, L. Callaghan, R. Ruby, and B. Otis, "A 50ppm 600MHz frequency reference utilizing the series resonance of an FBAR," in *2010 IEEE Radio Frequency Integrated Circuits Symposium*, IEEE, 2010.

[23] T. H. Lee, *The Design of CMOS Radio-Frequency Integrated Circuits*. Cambridge University Press, 2003.

[24] S. Razafimandimby, A. Cathelin, J. Lajoinie, A. Kaiser, and D. Belot, "A 2GHz 0.25um SiGe BiCMOS oscillator with flip-chip mounted BAW resonator," in *2007 IEEE International Solid-State Circuits Conference. Digest of Technical Papers*, IEEE, feb 2007.

[25] S. Rai and B. Otis, "A 1V 600uW 2.1GHz quadrature VCO using BAW resonators," in *2007 IEEE International Solid-State Circuits Conference. Digest of Technical Papers*, IEEE, feb 2007.

[26] D. Petit, E. Cesar, P. Bar, S. Joblot, G. Parat, O. Berchaud, J. Verdier, and J.-F. Carpentier, "Temperature compensated BAW resonator and its integrated thermistor for a 2.5GHz electrical thermally compensated oscillator," in *2009 IEEE Radio Frequency Integrated Circuits Symposium*, IEEE, jun 2009.

[27] J. Koo, K. Wang, R. Ruby, and B. P. Otis, "A 2-GHz FBAR-based transformer coupled oscillator design with phase noise reduction," *IEEE Transactions on Circuits and Systems II: Express Briefs*, vol. 66, pp. 542–546, apr 2019.

[28] R. Thirunarayanan, A. Heragu, D. Ruffieux, and C. Enz, "Complementary BAW oscillator for ultra-low power consumption and low phase noise," in *2011 IEEE 9th International New Circuits and systems conference*, IEEE, jun 2011.

[29] A. Rofougaran, J. Rael, M. Rofougaran, and A. Abidi, "A 900 MHz CMOS LC-oscillator with quadrature outputs," in *1996 IEEE International Solid-State Circuits Conference. Digest of Technical Papers, ISSCC*, IEEE.

[30] P. Andreani and X. Wang, "On the phase-noise and phase-error performances of multiphase LC CMOS VCOs," *IEEE Journal of Solid-State Circuits*, vol. 39, pp. 1883–1893, nov 2004.

[31] L. Romano, S. Levantino, A. Bonfanti, C. Samori, and A. Lacaita, "Phase noise and accuracy in quadrature oscillators," in *2004 IEEE International Symposium on Circuits and Systems (IEEE Cat. No.04CH37512)*, IEEE.

[32] Y.-C. Lo and J. Silva-Martinez, "A 5-GHz CMOS LC quadrature VCO with dynamic current-clipping coupling to improve phase noise and phase accuracy," *IEEE Transactions on Microwave Theory and Techniques*, vol. 61, pp. 2632–2640, jul 2013.

[33] S. Levantino, C. Samori, A. Bonfanti, S. Gierkink, A. Lacaita, and V. Boccuzzi, "Frequency dependence on bias current in 5 GHz CMOS VCOs: impact on tuning range and flicker noise upconversion," *IEEE Journal of Solid-State Circuits*, vol. 37, pp. 1003–1011, aug 2002.

[34] A. Ravi, K. Soumyanath, L. Carley, and R. Bishop, "An integrated 10/5GHz injection-locked quadrature LC VCO in a 0.18 um digital CMOS process," in *Proceedings of the 28th European Solid-State Circuits Conference*, pp. 543–546, 2002.

[35] S.-Y. Lee, L.-H. Wang, and Y.-H. Lin, "A CMOS quadrature VCO with sub-harmonic and injection-locked techniques," *IEEE Transactions on Circuits and Systems II: Express Briefs*, vol. 57, pp. 843–847, nov 2010.

[36] P. Tortori, D. Guermandi, E. Franchi, and A. Gnudi, "Quadrature VCO based on direct second harmonic locking," in *2004 IEEE International Symposium on Circuits and Systems (IEEE Cat. No.04CH37512)*, IEEE.

[37] S. Naseh, M. Z. Dooghabadi, and M. J. Deen, "A low-voltage low-noise super-harmonic quadrature oscillator," in *2008 15th IEEE International Conference on Electronics, Circuits and Systems*, IEEE, aug 2008.

[38] S. Gierkink, S. Levantino, R. Frye, and V. Boccuzzi, "A low-phase-noise 5GHz quadrature CMOS VCO using common-mode inductive coupling," in *Proceedings of the 28th European Solid-State Circuits Conference*, pp. 539–542, 2002.

[39] A. W. L. Ng and H. C. Luong, "A 1V 17GHz 5mW CMOS quadrature VCO based on transformer coupling," *IEEE Journal of Solid-State Circuits*, vol. 42, pp. 1933–1941, sep 2007.

[40] C.-W. Yao and A. Wilson, "A phase-noise reduction technique for quadrature LC-VCO with phase-to-amplitude noise conversion," in *2006 IEEE International Solid State Circuits Conference - Digest of Technical Papers*, IEEE, 2006.

[41] H.-R. Kim, C.-Y. Cha, S.-M. Oh, M.-S. Yang, and S.-G. Lee, "A very low-power quadrature VCO with back-gate coupling," *IEEE Journal of Solid-State Circuits*, vol. 39, pp. 952–955, jun 2004.